JEE Journal of Ecological Engineering

Journal of Ecological Engineering, 2026, 27(2), 277–292
https://doi.org/10.12911/22998993/211594
ISSN 2299–8993, License CC-BY 4.0

Received: 2025.09.14
Accepted: 2025.12.15
Published: 2026.01.15

Microplastic removal in coagulation-flocculation: Optimization through chemometric and morphological insights

Jareeya Yimrattanabovorn[1*], Kan Kanjanapruthipong[1], Watcharapol Wonglertarak[2], Boonchai Wichitsathian[1], Maturada Khowattana[1], Siriwan Nawong[3]

[1] School of Environmental Engineering, Institute of Engineering, Suranaree University of Technology, Nakhon Ratchasima 30000, Thailand
[2] Environmental Engineering and Disaster Management Program, Mahidol University, Kanchanaburi Campus, Kanchanaburi 71150, Thailand
[3] Synchrotron Research and Applications Division, Synchrotron Light Research Institute (Public Organization), Nakhon Ratchasima 30000, Thailand
* Corresponding author's e-mail: chareeya@sut.ac.th

ABSTRACT

Microplastics in freshwater threaten human health, making their removal in water treatment processes essential. Conventional coagulation methods, however, often show limited and inconsistent efficiency due to the diverse sizes, shapes, and surface properties of microplastics, underscoring the need for improved approaches. This study examined the removal performance, surface morphology, and chemical characteristics of polypropylene (MP-PP), polyethylene (MP-PE), and polystyrene (MP-PS) using poly-aluminum chloride (PAC) and anionic polyacrylamide (PAM) in a coagulation-flocculation process, with a focus on identifying optimal operating conditions. Among the tested microplastics, MP-PS exhibited the highest removal efficiency, followed by MP-PE and MP-PP, while larger particle size and mass were found to further enhance removal performance. Differences in removal efficiency were consistent with zeta potential values and supported by morphological evidence from scanning electron microscopy (SEM). Fourier transform infrared (FTIR) spectra, combined with Hierarchical Cluster Analysis (HCA) and Principal Component Analysis (PCA), further highlighted the influence of surface properties and aggregation behaviors on removal outcomes. Overall, the results demonstrate that optimizing parameters such as pH, coagulant dosage, polymer concentration, and consideration of microplastic characteristics can significantly enhance removal efficiency, providing practical guidance for advancing sustainable water treatment.

Keywords: microplastic, polypropylene, polyethylene, polystyrene, coagulation-flocculation processes, chemometric methods.

INTRODUCTION

The extensive use of plastics in packaging has resulted in the release of large quantities of plastic waste, significantly contributing to environmental pollution, particularly in water bodies. Through exposure to light, heat, and biological processes, larger plastic debris gradually fragments into particles smaller than 5 mm, known as microplastics (MP) (Collard et al., 2019; Eerkes-Medrano et al., 2015). Microplastics are now found in aquatic organisms, raising concerns about bioaccumulation (Zocchi and Sommaruga, 2019), and potential human health risks (Chae and An, 2019; Lei et al., 2018). While microplastics are commonly found in both marine and freshwater environments (Summers et al., 2018), freshwater environments warrant particular attention due to their direct connection to human water supplies (Stanton et al., 2020). Microplastics in freshwater ecosystems pose significant threats not only to human health but also to a wide range of aquatic organisms, including phytoplankton, zooplankton, fish, and aquatic birds. Moreover, microplastic

pollution can degrade water quality, thereby disrupting ecosystem function and biodiversity. The detection of microplastics in tap water (Tong et al., 2020), underscores the critical role of water treatment plants as barriers preventing these contaminants from reaching consumers. Among the various treatment processes, coagulation-flocculation represents a key mechanism for particle removal (Zhao et al., 2020), and has shown promise for microplastic removal (Skaf et al., 2020). The diversity of microplastics in freshwater systems (Xu et al., 2018b; Fu et al., 2020) presents challenges for treatment optimization, as removal efficiency varies significantly with particle characteristics (Ma et al., 2019b). Polypropylene (PP), polyethylene (PE), and polystyrene (PS) emerge as the most prevalent microplastic types in freshwater sources (Egessa et al., 2020; Huang et al., 2020; Yin et al., 2021), reflecting their extensive use in single-use packaging applications. Given their environmental prevalence, these three polymer types were selected as representative samples for this investigation.

The coagulation-flocculation process has proven effective in removing particles from water and remains a promising treatment option due to its low cost and ease of maintenance. Importantly, this process does not break down microplastics into smaller, potentially more hazardous fragments that could pose greater risks to human health and be more difficult to remove from water systems. Research has demonstrated that this process can aggregate small plastic particles into larger flocs (500–5.000 μm), achieving removal efficiencies of 98–99% under optimal conditions (Zhou et al., 2021). However, performance is highly dependent on microplastic characteristics including polymer type, particle size, and surface properties. Polyaluminum chloride (PAC) combined with anionic polyacrylamide (PAM) represents a widely implemented coagulant system in water treatment facilities (Ma et al., 2019b). This combination has demonstrated enhanced microplastic removal efficiency of up to 77.60% (Shahi et al., 2020; Zhang et al., 2021; Duan et al., 2022), with PAC and PAM forming bonds with MP particles to promote aggregation into rapidly settling flocs. The variation in reported efficiencies likely reflects differences in microplastic types, operating conditions, and water quality parameters across studies.

This study systematically evaluated the removal performance of different microplastic types (PP, PE, and PS) through the coagulation-flocculation process using PAC and PAM. The objectives were to: (1) assess the effectiveness of this process in removing microplastics, (2) investigate the factors affecting removal performance such as microplastic types, sizes, and optimal conditions, and (3) examine the relationship between removal efficiency and the morphological and chemical properties of microplastics before and after coagulation. Our findings provide key insights into how microplastic types, particle size, and morphology affect removal efficiency. They also offer practical recommendations for optimizing coagulation-flocculation processes for microplastic removal, contributing to sustainable water management.

MATERIALS AND METHODS

Preparation of microplastic samples

Polyethylene and polypropylene samples were obtained from Thantawan Industry, Thailand and polystyrene samples were obtained from Somboon Packaging (888) Company, Thailand. The samples were crushed to less than 5 mm using a blender (Philips Blender 3000 series, HR2041, China). The ground plastic samples were classified using the sieve analysis method (ASTM, 2004). The sieve sizes employed in this study adhered to ASTM standards, resulting in the categorization of plastic samples as MP-16 ($2.000 > x > 1.180$ μm), MP-40 ($1.180 > x > 425$ μm), and MP-60 ($425 > x > 250$ μm).

Chemicals added

Poly aluminum chloride (PAC) with molecular formula $Al_2(OH)_2Cl_6$ and purity 30% was obtained from Zhengzhou Megaman Chemical Limited, China. PAC is used as a coagulant in water treatment systems, particularly for municipal water production. An anionic polyacrylamide (PAM) with molecular formula $CH_2CHCONH_2$ was obtained from Welkin Enterprise, Thailand and used as the coagulant aid in this study.

Analysis of the physical and chemical characteristics of microplastic samples

After preparing the microplastic samples, particle size and shape analysis were carried out using the RODOS instrument, Qicpic model from

Germany. The analysis parameters were fiber length (LEFI), fiber diameter (DIFI), and straightness, with elongation calculated using Equation 1, The accuracy of the results was validated in collaboration with The Kittisit Enterprise in Germany and Thailand. The microplastic samples were analyzed before and after the coagulation-flocculation process for their morphological characteristics using a Scanning Electron Microscope (SEM) JEOL JSM-6010LV model from Japan. The zeta potential was measured using a Malvern ZS nanoparticle instrument from the UK, and the functional groups of the microplastic samples were identified through Fourier transform infrared spectroscopy (FTIR) with a Bruker Tensor 27 model from Germany.

$$Elongation = \frac{DIFI}{LEFI} \quad (1)$$

where: $DIFI$ – fiber diameter, $LEFI$ – fiber length.

Coagulation-flocculation experiments

The experimental setup comprised a Wizard PLUS 6 LED Jar Test machine from Germany. Each coagulation experiment was conducted using 1.000 mL of deionized (DI) water. The study conditions included rapid mixing at 300 rpm (G=358 sec^{-1}) for 1 minute, followed by slow mixing at 100 rpm (G=74 sec^{-1}) for 15 minutes, and a 30-minute sedimentation period at room temperature (Ma et al., 2019b).

The experiments were conducted in two phases. In the first phase, the microplastic concentration was maintained at 0.10000 ± 0.00500 g per 1.000 mL of DI water to investigate the effects of PAC concentration, PAM concentration, and initial pH on removal efficiencies. Detailed experimental conditions for each type of microplastic sample (PP, PE, and PS) with particle size MP40 are shown in Table 1.

In the second phase, subsequent experiments explored how variations in particle size (MP16, MP40, and MP60) and microplastic concentration (ranging from 0.02500 to 0.15000 g per 1.000 mL of DI water) influenced removal efficiencies for the three microplastic types (PP, PE, and PS). The coagulation-flocculation process conditions (PAC concentration, PAM concentration, and initial pH) used in these size and concentration variation experiments were based on the optimal conditions determined from the first phase.

Data analysis

After sedimentation by coagulation-flocculation, the floating microplastic samples were collected from the surface using a 50 mL syringe with approximately 200 mL of water from the surface, representing the non-sedimented microplastics (Arvaniti et al., 2021; Peller et al., 2022). The collected water samples were filtered using Whatman GF/C Glass circles with a pore size of 47 microns (Zhou et al., 2021). The non-sedimented microplastic samples were soaked in 1M HCl for 30 minutes in a volume of 5 mL to remove PAC and PAM (Zhang et al., 2021) After acid treatment, the samples were filtered again, rinsed with DI water, and dried in a hot air oven at 105 °C for 12 hours. X_0 and X_e as initial and non-sedimented microplastic samples(g) were weighed using a Semi-Micro Analytical Balance (ML-series, Mettler Toledo, Switzerland) with a precision of five decimal places. The microplastic removal efficiency through the coagulation-flocculation process was then calculated using Equation 2.

$$Removal\ efficiency\ (\%) = \frac{X_0 - X_e}{X_0} \times 100 \quad (2)$$

where: X_0 – initial microplastic(g) and X_e – non sedimented microplastic(g).

HCA and PCA

Fourier-transform infrared spectra from the MP samples, collected before and after coagulation, were processed using OPUS 7.5 (Bruker Optics Ltd., Ettlingen, Germany). This process included smoothing (20 points), baseline correction, and vector normalization. Hierarchical cluster analysis (HCA) and principal component analysis (PCA) were then conducted using Unscrambler

Table 1. Detailed coagulation-flocculation process experiments for different types of microplastic samples

Experiments for different types of microplastics	PAC concentration (mg/L)	PAM concentration (mg/L)	Initial pH
Effect of PAC	20–160	10	7.0–7.5
Effect of PAM	Results from Exp no.1	2–16	7.0–7.5
Initial pH	Results from Exp no.1	Results from Exp no.2	5.0–12.0

X 10.5 software (64-bit, CAMO Software AS, Norway). These chemometric techniques visualized the clustering of the analyzed samples, while PCA highlighted spectroscopic changes and differences among the MP samples. The PCA results were displayed as a score plot providing a graphical representation, and a loading plot identifying specific spectroscopic changes.

RESULTS AND DISCUSSION

Physical characteristics of microplastic samples

The microplastic samples were categorized by size (MP16, MP40, MP60) and analyzed using the RODOS instrument (Table 2). For PP, more than 80% of the samples had elongation values below 0.20, indicating low symmetry and minimal sphericity. MP60-PP, the smallest size, was the most spherical, while MP16-PP had the lowest straightness values (0.520–0.823), suggesting reduced linearity. LEFI and DIFI values were most pronounced in MP16-PP, showing more uniform shapes as size decreased. These results are consistent with Julian et al., 2023, who reported filament-like morphology in ground polypropylene microplastics.

PE samples showed elongation values mostly below 0.50, indicating better spherical symmetry than PP. MP60-PE was the most spherical, followed by MP40-PE and MP16-PE. Straightness values were lowest for MP16-PE (0.780–0.891) but increased with larger sizes, indicating greater linearity. LEFI and DIFI values also reflected more symmetrical shapes at smaller sizes, in agreement with Wagner et al., 2014, who observed rounded or subrounded polyethylene microplastics in river samples.

PS samples exhibited elongation values mostly below 0.40, reflecting higher spherical symmetry than PP but slightly lower than PE. MP60-PS was the most spherical, with straightness values ranging from 0.858 to 1.000, compared to 0.837–0.916 for MP16-PS. Increasing symmetry between LEFI and DIFI with decreasing size indicated more spherical shapes, consistent with Colombi et al., 2009.

The zeta potential measurements of the microplastic samples gave polypropylene -3.57 mV, polyethylene -5.26 mV, and polystyrene -6.60 mV. These negative zeta potential values indicated that the surfaces of the microplastics carried a negative charge and behaved as colloidal particles in water. They were effectively removed through coagulation which neutralized the surface charge of the particles, facilitating their aggregation and removal from the aqueous solution.

Optimal conditions for microplastic removal using the coagulation-flocculation process

As shown in Figure 1a, there was a significant increase in the removal efficiency of all microplastic types as the PAC concentration increased from 20 mg/L to 100 mg/L. The removal efficiency rose from 5.59% to 14.83% for MP40-PP, from 6.50% to 16.54% for MP40-PE, and from 7.00% to 18.23% for MP40-PS. Increasing the PAC concentration beyond 100 mg/L up to 160 mg/L led to a decline in removal efficiencies to 9.20% for MP40-PP, 9.20% for MP40-PE, and 9.77% for MP40-PS. These findings indicated that the optimal PAC concentration for achieving maximum removal efficiency of MP40 microplastics was 100 mg/L. This trend was explained by changes in the zeta potential of PAC. The detailed zeta potential results are presented in Table 3. When PAC was dissolved in water, the zeta potential increased from +4.00 mV at 20 mg/L to +16.30 mV at 100 mg/L, but further increasing the concentration to 160 mg/L reduced it to +6.37 mV. This behaviour was due to the dissociation of more positive ions at higher PAC concentrations, leading to the release of H^+ ions and a decrease in the pH of the water. As the pH decreased, PAC formed negatively charged complexes like $Al(OH)_4^-$ and $Al(OH)_5^{2-}$, rather than $Al(OH)_3$, which is essential for effective sweep coagulation and sedimentation. At pH levels below 4.5, PAC hydrolysis was inhibited, reducing its effectiveness in coagulating and settling the colloidal particles (Wei et al., 2015).

A similar trend was observed with the PAM concentrations, as illustrated in Figure 1b, Increasing the PAM concentration from 2 mg/L to 14 mg/L enhanced the removal efficiencies for both MP40-PP and MP40-PE, with MP40-PP rising from 6.72% to 20.59% and MP40-PE from 6.24% to 21.63%. When the PAM concentration was increased to 16 mg/L, the removal efficiency dropped to 18.51% for MP40-PP and 19.70% for MP40-PE. By contrast, the removal efficiency of MP40-PS increased from 6.54% to 22.63% as the PAM concentration increased from 2 mg/L to 12 mg/L while a further increase to 16 mg/L reduced

Table 2. Characteristics of microplastic type and particle size. (n = 3)

Type and particle size of microplastic	Morphology	Straightness	Elongation	Diameter (μm)	
				LEFI	DIFI
MP16-PP		0.520–0.823	0.011–0.082	8,696.414–11,186.853	91.742–825.383
MP40-PP		0.728–0.935	0.018–0.063	4,813.181–9,806.691	140.121–450.499
MP60-PP		0.729–0.971	0.027–0.110	1,169.662–8,610.458	128.293–265.516
MP16-PE		0.780–0.891	0.087–0.177	2,670.633–5,662.617	473.498–739.118
MP40-PE		0.802–0.951	0.125–0.307	1,094.514–2,559.928	313.110–391.773
MP60-PE		0.874–1.000	0.226–0.394	405.322–693.178	101.031–174.533
MP16-PS		0.837.0.916	0.096–0.227	1,630.454–3,031.244	242.561–370.481
MP40-PS		0.858–0.955	0.130–0.267	709.236–1,166.452	116.863–248.229
MP60-PS		0.857–1.000	0.216–0.494	116.850–928.899	82.359–200.600

the efficiency to 18.48%. These results were explained by changes in the zeta potential of the PAM, which became more negative as the concentration increased from -14.90 mV at 2 mg/L to -38.80 mV at 16 mg/L. The dissolved PAM, imparting a negative charge on the organic components, with the number of negative charges depending on the amount of dissolved acrylamide groups.

The optimal microplastic removal efficiency at PAM concentrations of 12–14 mg/L resulted from the electrochemical balance between the positively charged PAC and negatively charged PAM. At these concentrations, the charge neutralization was most effective, creating favorable conditions for destabilization of microplastic particles. Beyond 14 mg/L PAM concentration, despite further increases in negative zeta potential, the removal efficiency decreased due to charge reversal and restabilization of the colloidal system. The excess negative charges from higher PAM concentrations overcame the positive charges from PAC, leading to electrostatic repulsion rather than attraction between particles

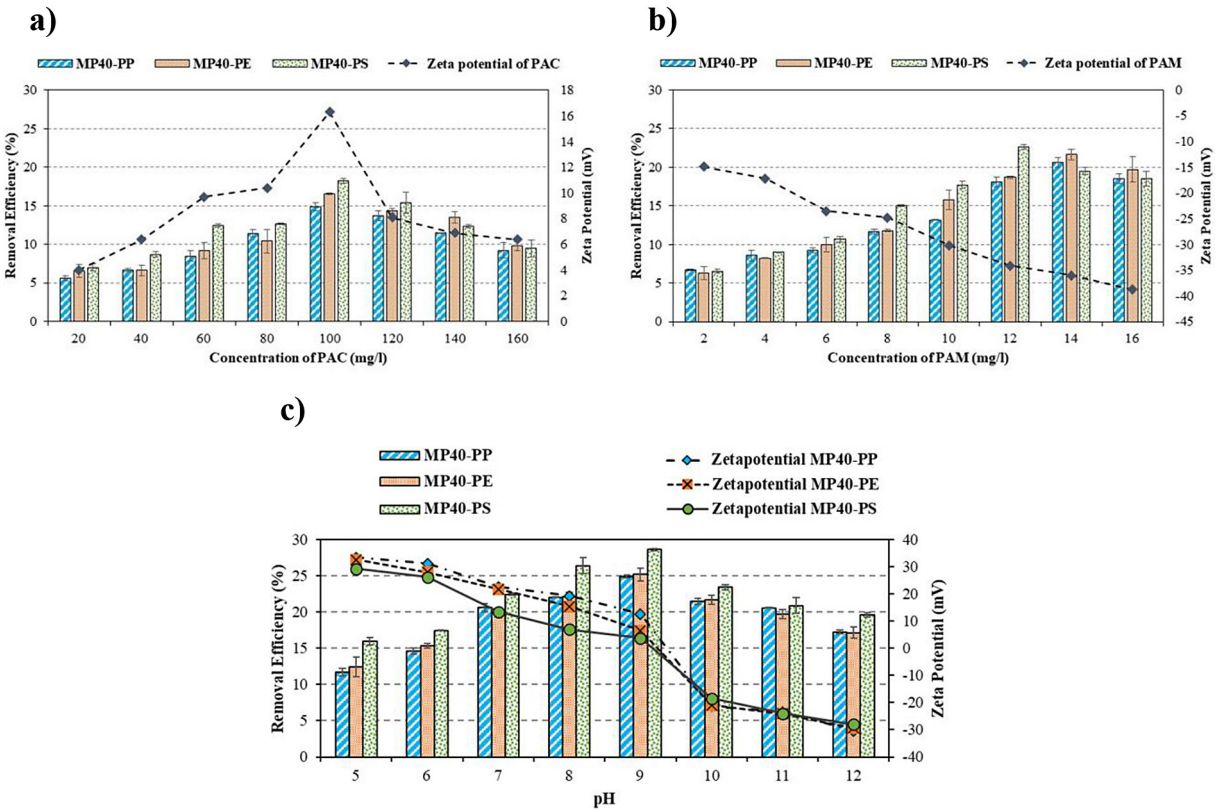

Figure 1. Influence of coagulation-flocculation parameters on microplastic removal efficiency at (a) PAC concentration variation, (b) PAM concentration variation, (c) effect of pH variation

Table 3. Zeta potential of PAC and PAM at different concentrations

PAC		PAM	
Concentration (mg/l)	Zeta potention (mV)	Concentration (mg/l)	Zeta potention (mV)
20	+4.00	2	-14.90
40	+6.37	4	-17.20
60	+9.69	6	-23.50
80	+10.40	8	-24.80
100	+16.30	10	-30.20
120	+8.08	12	-34.10
140	+6.87	14	36.00
160	+6.37	16	-38.80

and coagulant/flocculant complexes. Furthermore, PAM functioned as a flocculant aid through bridging mechanisms, connecting destabilized colloidal particles to enhance settling (Wiśniewska et al., 2015). However, at excessive PAM concentrations, the predominance of negative charges disrupted this bridging effect, explaining why removal efficiency declined even as individual zeta potential values continued to change.

This demonstrates that in dual coagulant-flocculant systems, the removal efficiency depends on the synergistic electrochemical interactions between both components rather than the zeta potential of individual chemicals alone.

The effect of pH on microplastic removal efficiency through the coagulation-flocculation process is illustrated in Figure 1c, increasing the pH from 5 to 9 improved the removal efficiency, with MP40-PP rising from 11.69% to 24.86%, MP40-PE from 12.40% to 25.19%, and MP40-PS from 15.96% to 28.59%. When the pH was increased from 9 to 12, the removal efficiency decreased, dropping to 17.24% for MP40-PP, 17.11% for MP40-PE, and 19.60% for MP40-PS. These results

were consistent with the changes in zeta potential following the coagulation-flocculation process. As the pH increased from 5 to 9, the zeta potential approached zero (neutralization), with MP40-PP decreasing from +33.40 mV to +12.60 mV, MP40-PE from +32.50 mV to +6.50 mV, and MP40-PS from +29.20 mV to +3.69 mV. This trend aligned with the observed increase in removal efficiency. When the pH increased from 9 to 12, the zeta potential became more negative, in line with the decreased removal efficiency of microplastics.

PAC demonstrated effective removal of colloidal particles within a pH range of 5.0 to 9.0, with optimal coagulation performance between pH 6.0 and 9.5. The present study's results align with this established range, showing maximum removal efficiencies at pH 9 for all MP40 microplastics: 24.86% for MP40-PP, 25.19% for MP40-PE, and 28.59% for MP40-PS. The superior performance at pH 9 can be attributed to favorable electrochemical interactions between PAC and the microplastic particles.

The zeta potential of the microplastics exhibited significant pH-dependent variation (Supplementary Table 4). As pH increased from 5 to 12, all microplastic types became increasingly negative: MP40-PP decreased from +2.72 to -21.00 mV, MP40-PE from +1.56 to -23.40 mV, and MP40-PS from +4.00 to -14.10 mV. This pH-dependent charge variation directly influenced the electrostatic interactions with PAC species.

At pH levels below 6, PAC forms positively charged complexes such as Al^{3+} and $Al(OH)_2^+$, which exhibit strong adsorption onto colloidal particles. This interaction increases particle stability and elevates the positive zeta potential, thereby reducing removal efficiency (Kabsch-Korbutowicz, 2005; Wei et al., 2015). Conversely, above pH 9, PAC forms negatively charged complexes including $Al(OH)_4^-$ and $Al(OH)_5^{2-}$, which electrostatically repel the negatively charged colloidal particles. This repulsion increases the magnitude of negative zeta potential, stabilizes the colloids, and consequently decreases removal efficiency (Chavalparit and Ongwandee, 2009).

Hierarchical cluster analysis is a technique used to group data into subgroups based on their similarities or differences (Pedro and Fionn, 2015), offering insights into the relationships between variables. In this study, microplastic samples before and after the coagulation-flocculation process, under various pH conditions, were analyzed using FTIR spectroscopy. HCA was employed to visualize the clustering of MP-PP, MP-PE, and MP-PS, as shown in Figure 2a, Figure 2b, and Figure 2c, respectively. The analysis utilized Ward's algorithm with standard Euclidean distance and considered frequency ranges of 399–3996 cm^{-1}. Three clusters were identified in the HCA analysis of all microplastic types as (1) MP samples before coagulation-flocculation, (2) MP samples after coagulation-flocculation with the most effective reactions, and (3) MP samples after coagulation-flocculation with minimal reactions.

Cluster (1) exhibited the least correlation, representing samples that had not undergone the coagulation-flocculation process and lacked functional groups associated with it. By contrast, clusters (2) and (3) were closely related, as both had undergone the coagulation-flocculation process. The functional groups Al-O, C=O, and OH- were detected on the surface of the microplastics after coagulation-flocculation. Notably, cluster (3) included samples treated at pH 9 for all microplastic types, demonstrating the highest removal efficiencies. These findings suggested that pH 9 was optimal for maximizing microplastic removal for all the microplastic types.

Table 4. Zeta potential results of MPs under varying pH conditions

pH	Zeta potention (mV)		
	MPpp-40	MPpe-40	MPps-40
5	+2.72	+1.56	+4.00
6	+0.106	-2.17	+3.62
7	-3.57	-5.26	-6.60
8	-5.20	-6.27	-7.92
9	-6.09	-6.75	-9.35
10	-9.98	-9.19	-11.50
11	-13.70	-16.30	-12.60
12	-21.00	-23.40	-14.10

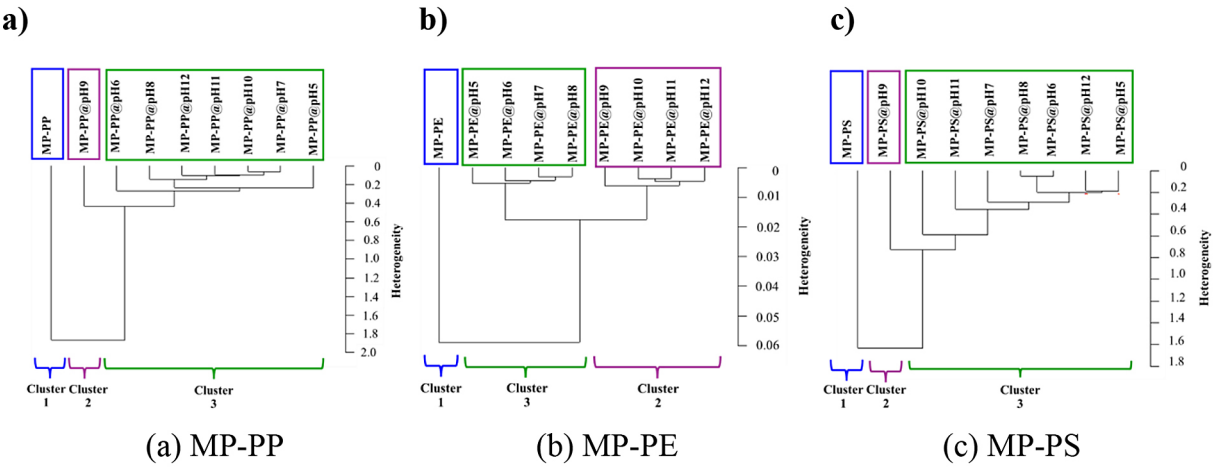

Figure 2. Hierarchical cluster analysis HCA of pH variation at: (a) MP-PP, (b) MP-PE, (c) MP-PS

Effect of microplastic size and mass on removal efficiency

Results in Figure 3, demonstrated that the removal efficiency improved as the size of the microplastics increased, progressing from MP60 to MP40, and then to MP16. The removal efficiency for MP-PP microplastics was 21.88%, 24.90%, and 26.39%, respectively. Similarly, MP-PE exhibited removal efficiencies of 22.59%, 25.40%, and 28.73%, while MP-PS showed removal rates of 23.08%, 28.50%, and 30.11% for the corresponding sizes. Increasing the size of microplastics from MP60 to MP40 and MP16 disrupted the dispersion layer more effectively, bringing the zeta potential closer to zero. Larger microplastics are generally less stable than smaller ones, as they more easily aggregate into larger flocs, which enhances removal efficiency. Larger particles have a greater potential for flocculation and sedimentation, exerting stronger compressive forces compared to smaller particles (Zhang et al., 2021). In this study, the zeta potential after the coagulation-flocculation process revealed that larger microplastic sizes gave zeta potentials closer to zero. The zeta potentials for microplastic sizes MP60, MP40, and MP16 were +24.90, +12.60, and +11.80 mV for PP, +14.30, +9.46, and +7.66 mV for PE, and +13.40, +10.60, and +6.50 mV for PS, respectively. These findings concurred with Shahi et al., 2020, who reported that larger polyethylene microplastics exhibited higher removal efficiencies due to their greater instability compared to smaller ones. This finding was also supported by

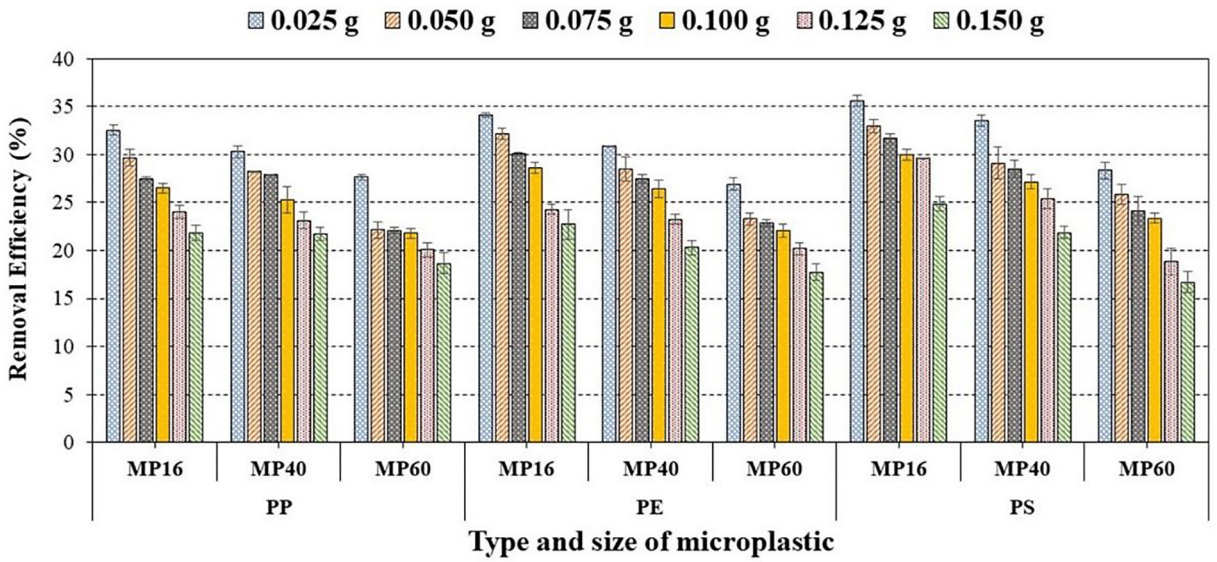

Figure 4. Effect of microplastic mass and size on removal efficiency

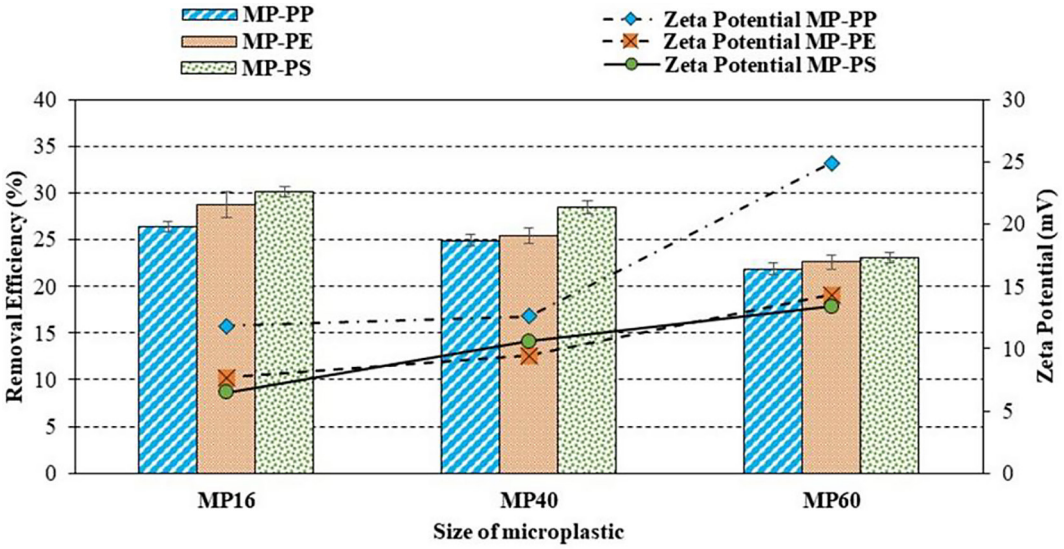

Figure 3. Effect of microplastic size on removal efficiency

Pivokonsky et al., 2018, who observed that smaller polyethylene microplastics were less efficient in the removal processes due to their higher quantity and insufficient destabilization.

Results in Figure 4, indicated that increasing the microplastic mass from 0.025 g/L to 0.150 g/L decreased the removal efficiency for all types of microplastics. The removal efficiency of MP16-PP dropped from 32.56% to 21.85%, MP16-PE decreased from 34.12% to 22.73%, and MP16-PS fell from 35.63% to 24.84%. These results were consistent with changes in microplastic size. As the microplastic size decreased from MP16 to MP60, the removal efficiency declined because the optimal coagulant dosage was inversely related to the colloid concentration. Water with lower turbidity requires a higher amount of coagulant to achieve effective coagulation, while water with higher turbidity requires less coagulant due to increased particle interactions. When the microplastic mass increased from 0.025 to 0.150 g/L, the removal efficiency decreased. Conversely, when the microplastic size increased from MP60 to MP16, the removal efficiency decreased. Due to that larger size microplastics (MP16) had fewer particles number compared to smaller size microplastics (MP40 and MP60). The reason is that water samples with a higher number of microplastic particles require a larger amount of coagulant to achieve effective coagulation, while water samples with fewer microplastic particles require the optimal amount of coagulant, leading to improved coagulation efficiency.

Morphology of microplastics in the coagulation-flocculation process

The morphological analysis of microplastic samples was conducted using SEM to examine changes before and after coagulation Figure 5 Before coagulation, MP-PP exhibited flat, linear structures with hard, rough surfaces, straight edges, and numerous scratches Figure 5a, These observations concurred with Lin et al., 2015 and Moura et al., 2023, who reported similar features in polypropylene microplastics. After coagulation, MP-PP developed a softer, fluffier texture with increased density, fibrous structures, and numerous small surface particles Figure 5b, consistent with Adib et al., 2022. Similarly, MP-PE displayed an uneven surface with curved and irregular edges, rough texture, and fissure-like scratches before coagulation, giving it a wavy appearance Figure 5c, This is consistent with Weinstein et al., 2016, who described polyethylene microplastics as having rough surfaces with pits and cracks. Following coagulation, MP-PE exhibited a smoother surface with reduced curvature, more uniform coatings, fibrous structures, and numerous small particles Figure5d, in agreement with Zhou et al., 2021.

In comparison, MP-PS initially showed a wavy surface with curved edges and a relatively smooth texture Figure 5e. After coagulation, MP-PS developed a rougher, more porous surface enriched with small particles Figure 5f. These changes demonstrate that coagulation substantially alters the surface morphology of all three MPs, producing softer textures and enhancing particle

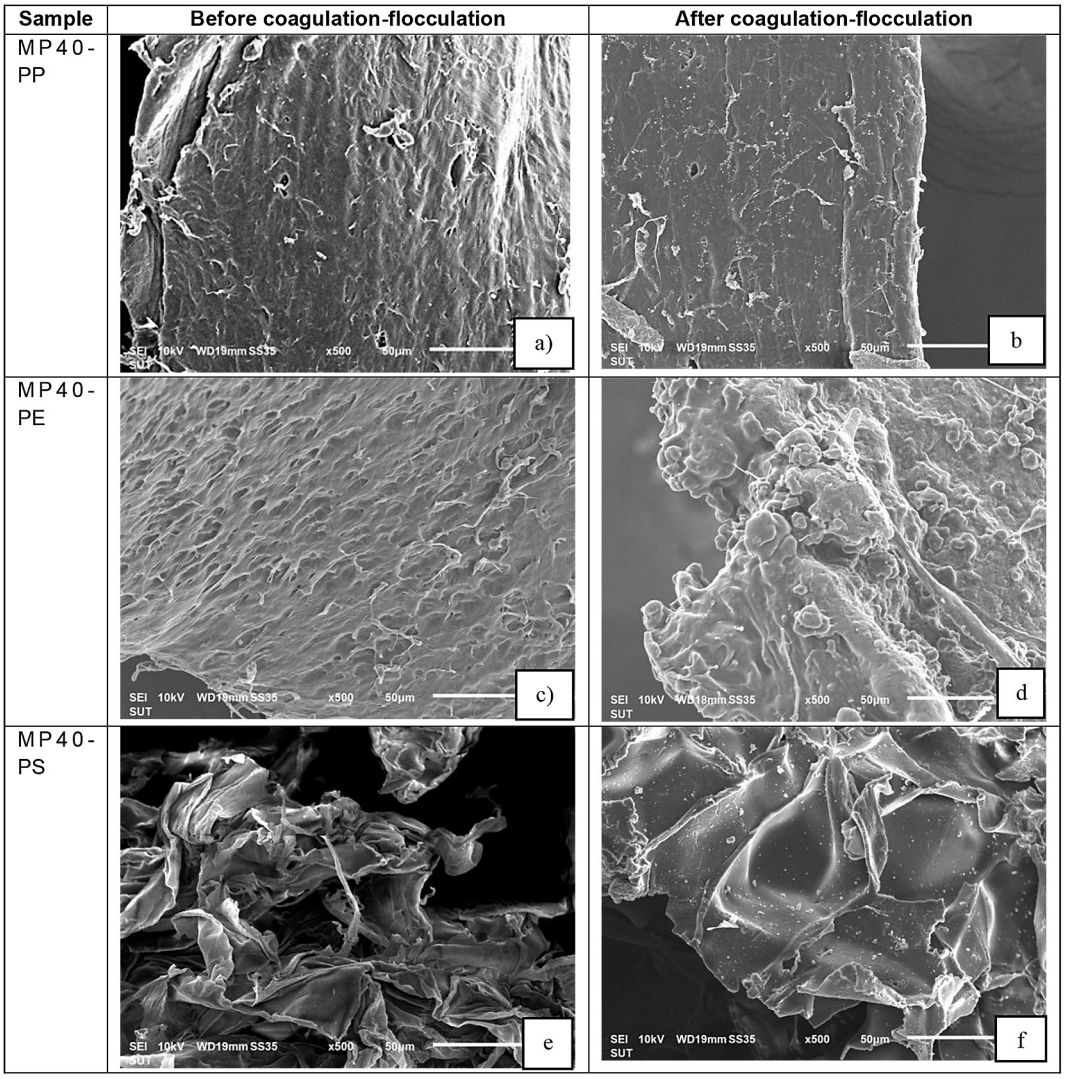

Figure 5. Morphology of microplastics before and after coagulation-flocculation by scanning electron microscopy at 500 times magnification (a) MP40-PP before coagulation, (b) MP40-PP after coagulation, (c) MP40-PE before coagulation, (d) MP40-PE after coagulation, (e) MP40-PS before coagulation, and (f) MP40-PS after coagulation

deposition. Overall, particle size and shape analysis revealed distinct differences among the three polymers: PS exhibited the most symmetrical shapes, PE displayed intermediate symmetry with greater linear length, and PP showed the least symmetry with narrower widths. These morphological characteristics, including roughness and sphericity, are critical factors influencing coagulation and removal efficiency.

The results explained why MP-PS showed the highest removal efficiency compared to MP-PP and MP-PE, supporting the idea that rough surfaces improve removal efficiency by providing more surface area and better adhesion (Jiang et al., 2006). These findings were consistent with Hassan et al., 2016, who observed that rough microplastics were removed more effectively due to increased aggregation and settling compared to smoother particles. Rough particles are less stable and aggregate more easily, resulting in enhanced sedimentation (Jiang et al., 2006). These observations aligned with studies indicating that coagulation alters microplastic surfaces, promoting the formation of small particles and potentially contributing to a foam-like structure due to interactions between coagulants and microplastic particles (Gandurina and Gervite, 1987; Zhou et al., 2021; Zhang et al., 2021).

Chemical properties of microplastics in the coagulation-flocculation process

FTIR analysis of functional groups in PAC, PAM, and microplastic samples, conducted before

and after the coagulation-flocculation process revealed several key findings. As illustrated in Figure 6, PAC displayed hydroxyl groups (-OH) associated with aluminum, formed through the hydrolysis of PAC in the presence of OH^- ions from water. This was evidenced by O-H bond stretching at wavenumbers 3200–3600 cm^{-1} and O-H bond bending at wavenumbers 1600–1650 cm^{-1} (Yang et al., 2011; Zhao et al., 2022). The Al-O functional group, a critical component of PAC, was identified at wavenumbers 400–700 cm^{-1}, indicating aluminum-oxygen bonding. In the analysis of PAM, the carbonyl group (-C=O) was observed with stretching at wavenumbers 1650–1690 cm^{-1}. N-H bond bending, and C-N stretching were detected at wavenumbers 1540–1560 cm^{-1}. The amino group ($-NH_2$), characteristic of amides, along with methylene groups ($-CH_2-$) in the carbon chain, appeared at wavenumbers 1380–1450 cm^{-1} (Silverstein et al., 2005).

As shown in Figure 6a, hydrocarbon groups (C-H), typical of alkane compounds, were detected in MP-PP before the coagulation-flocculation process. These included specific deformations in the CH_2 and CH_3 groups, characteristic of polypropylene. After the coagulation-flocculation process, the presence of these hydrocarbon groups (C-H) and the deformations in CH_2 and CH_3 remained unchanged, indicating that the fundamental structure of polypropylene was preserved. New absorption bands appeared at 1600–1700 cm^{-1}, corresponding to amide spectra, suggesting interactions between the PAM and PAC, leading to flocculation of the microplastic particles. The absorption bands at 600–700 cm^{-1}, indicated the formation of new Al-O bonds between the microplastics and PAC. The absence of these bands before the coagulation-flocculation process confirmed the successful modification of the microplastic surface through the treatment (Wang et al., 2020; Luo et al., 2021; McYotto et al., 2021; Zhou et al., 2021).

Before the coagulation-flocculation process, FTIR analysis of MP-PE, shown in Figure 6b, revealed hydrocarbon groups (C-H) and primarily alkanes, characteristic of polyethylene, as reported by Gulmine et al., 2022 and Tabatabaei et al., 2023. The hydrocarbon groups in MP40-PE exhibited distinct deformation and bending similar to those found in polypropylene, but with different absorption bands. MP-PE displayed absorption bands in the 2800–2900 cm^{-1} range,

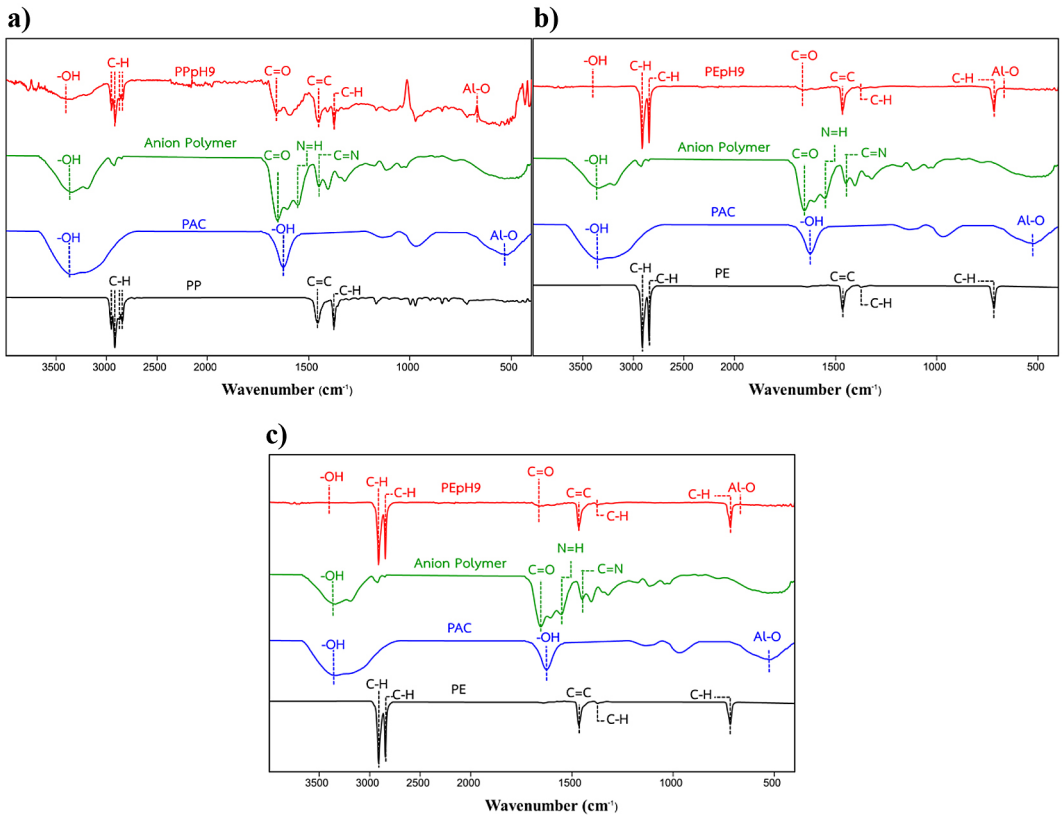

Figure 6. Analysis of functional groups in three types of microplastic samples using FTIR after the coagulation process at: (a) PP, (b) PE and (c) PS

compared to MP-PP, which exhibited bands in the 2800–3000 cm^{-1} range. After the coagulation-flocculation process, FTIR analysis indicated that the functional groups of MP-PE, including the hydrocarbon groups and their deformations, remained largely unchanged. The new absorption bands at 1600–1700 cm^{-1} were indicative of amide spectra, signaling interactions between PAM and PAC, which facilitated the flocculation process. The absorption bands at 600–700 cm^{-1} suggested the formation of new Al-O bonds between the microplastics and PAC. The absence of these bands before the coagulation-flocculation process confirmed that the surface modification of the microplastics was effectively achieved (Wang et al., 2020; McYotto et al., 2021; Zhou et al., 2021).

As shown in Figure 6c, FTIR analysis of MP-PS microplastics before the coagulation-flocculation process revealed hydrocarbon groups (C-H) characteristic of both aromatics and alkanes, with a distinct peak for the aromatic (C=C) component, setting them apart from MP-PP and MP-PE. MP-PS exhibited a specific structure with benzene rings, indicated by out-of-plane bending of C-H (Fang et al., 2010; Zhou et al., 2021). After the coagulation-flocculation process, the functional groups of polystyrene microplastics remained largely unchanged, with hydrocarbon groups (C-H) related to aromatics and alkanes, and the aromatic (C=C) component and out-of-plane C-H bending still present. New absorption bands at 1600–1700 cm^{-1}, were characteristic of amide spectra, indicating interactions between PAM and PAC, leading to hydrolysis of the microplastic particles (Luo et al., 2021). The absorption bands at 600-700 cm^{-1} suggested the formation of new Al-O bonds between the microplastics and PAC. The absence of these bands before the coagulation-flocculation process confirmed that surface modification of the microplastic occurred effectively (Wang et al., 2020; McYotto et al., 2021; Zhou et al., 2021).

PCA of three types of microplastic samples in the coagulation-flocculation process

PCA was conducted to identify changes in the MP samples and differentiate among the three types before and after coagulation to provide comprehensive insights. The results were visually represented through score plots, based on the principal components, alongside loading plots that displayed their spectral characteristics.

Chemometric methods demonstrated the separation of MP-PP, MP-PE, and MP-PS microplastics types before the coagulation-flocculation process. As shown in Figure 7a and Figure 7b the PCA plots displayed a clear separation into three distinct branches. PC1 Figure 7c, accounted for 84% of the variance, effectively distinguishing MP-PP from MP-PE and MP-PS, while PC2 Figure 7d, accounted for 16% of the variance, differentiating MP-PS from MP-PP and MP-PE. The loading plot for PC1 indicated that MP-PP showed the greatest difference from MP-PE and MP-PS at 2916.15 cm^{-1} (asymmetric CH_2 stretching) and 2848.66 cm^{-1} (symmetric CH_2 stretching), characteristic bands of MP-PE. Differences were also noted at 1465.79 cm^{-1} (CH_2 scissoring in alkanes) and 717.47 cm^{-1} (CH_2 rocking), although these variations were smaller than the previously mentioned positions. Other distinctions corresponded to characteristic bands of PP at 2952.80 cm^{-1} (CH_3 stretching in alkanes), 1375.15 cm^{-1} (CH_3 stretching in alkanes), 1166.85 cm^{-1} (C-H wagging in alkanes), 997.13 cm^{-1} (CH_3 rocking in alkanes), 972.05 cm^{-1} (C–C stretching), and 840.90 cm^{-1} (CH_2 rocking). In the loading plot for PC2 of the MP samples, MP-PS displayed the largest difference from MP-PP and MP-PE at 1375.15 cm^{-1} (CH_3 stretching in alkanes) and 2835.15 cm^{-1} (CH_3 stretching), characteristic bands of MP-PP and MP-PE, respectively. Other notable differences for MP-PP included bands at 2950.88 cm^{-1} (CH_3 stretching in alkanes), 2867.94 cm^{-1} (CH_3 stretching), 1166.85 cm^{-1} (C-H wagging in alkanes), 997.13 cm^{-1} (CH_3 rocking in alkanes), 972.05 cm^{-1} (C–C stretching), and 840.90 cm^{-1} (CH_2 rocking). For MP-PE, characteristic bands were observed at 2923.87 cm^{-1} (C-H stretching in alkanes) and 1456.15 cm^{-1} (C=C stretching in aromatics). By contrast, MP-PS exhibited bands at 1481.22 cm^{-1}, 1456.15 cm^{-1} (C=C stretching), 707.82 cm^{-1} (C-H out-of-plane bending in aromatics), and 682.75 cm^{-1} (C-H out-of-plane bending in aromatics) (Amelia et al., 2022; Mikulec et al., 2023).

PCA revealed that MP-PE, MP-PP, and MP-PS exhibited both similarities and differences in their bonding characteristics. Distinctive bonds that set MP-PE apart from the other two types included symmetric CH_2 stretching at 2848.65 cm^{-1} and CH_2 scissoring at 1467.72 cm^{-1}. For MP-PP, the differentiating bond was C–C stretching, observed at 960.48 and 985.55 cm^{-1}. By contrast, PS was distinguished by C=C stretching (1451–1492

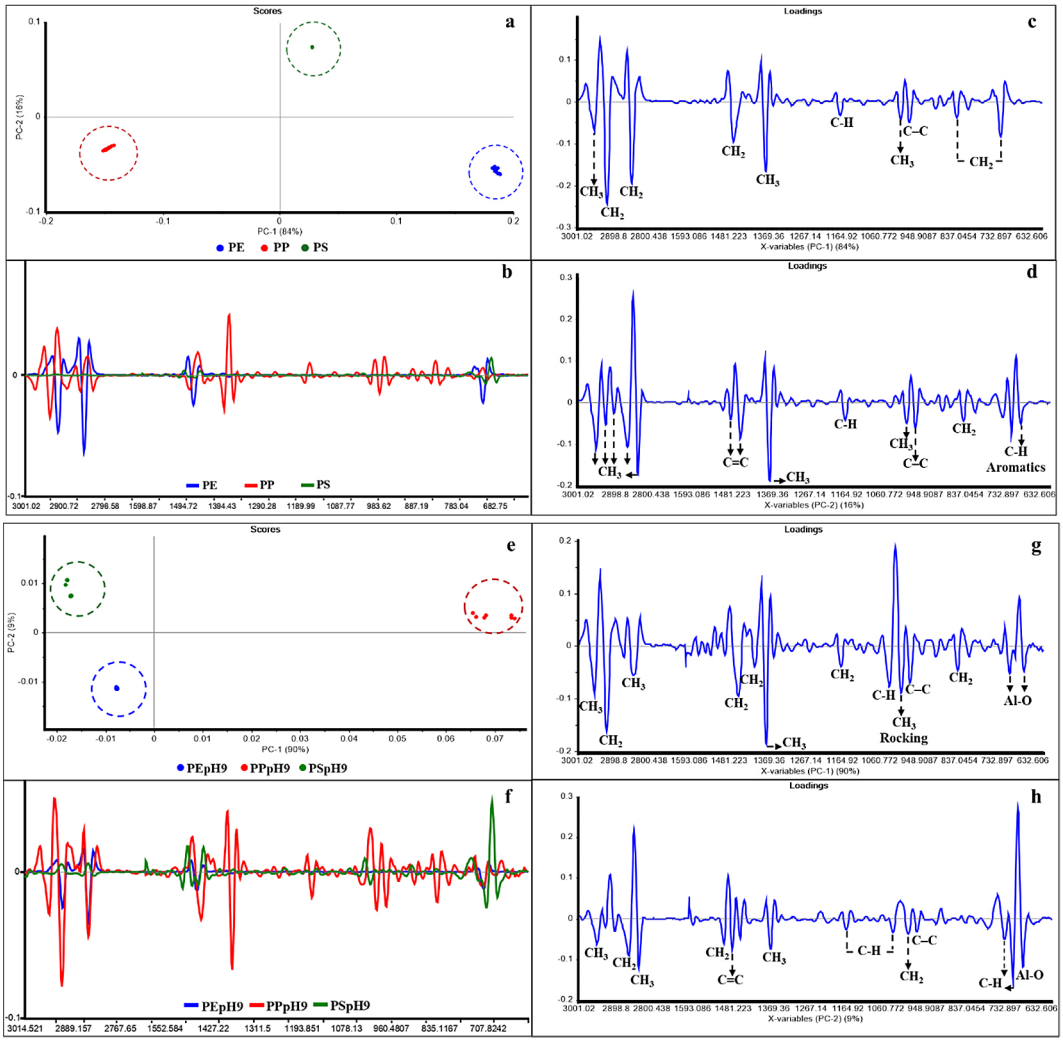

Figure 7. Analysis of groups in three types of microplastic samples using PCA before (a-d) and after (e-h) the coagulation process (a, e) PC1 and PC 2 map, (b, f) line plots of microplastic samples, (c, g) loading plots of PC 1, and (d, h) loading plots of PC 2

cm^{-1}) and C-H out-of-plane bending in aromatics (690–754 cm^{-1}). Similarities between MP-PE and MP-PP were reflected in the CH_2 rocking bands at 717.47 and 719.31 cm^{-1}, as well as asymmetric CH_2 stretching at 2914.23 and 2937.37 cm^{-1}. The similarity between MP-PP and MP-PS was attributed to the CH_3 stretching bonds, ranging from 2825.51 to 2893.01 cm^{-1} and 2848 to 2920 cm^{-1}. These findings aligned with Mikulec et al., 2023.

FTIR spectra analysis of the MP samples after the coagulation-flocculation process revealed a clear and consistent separation into three distinct branches, as illustrated in Figure 7e and Figure 7f, similar to the pre-process observations. In Figure 7g PC1 had a 90% distinction between MP-PP and the other two types, MP-PE and MP-PS. Fig. 7h showed PC2, highlighting a 9% distinction for MP-PE from MP-PP and MP-PS, as illustrated in the PCA score plots. The loading plot of PC1 for microplastics showed that MP-PP differed from MP-PE and MP-PS at the same bond positions observed before the coagulation-flocculation process. Notable differences appeared at specific positions including CH_2 alkane stretching at 1407.934 cm^{-1}, C-H alkane wagging at 1031.842 cm^{-1}, and Al-O bond positions at 696.2522 cm^{-1} and 657.6787 cm^{-1}. These findings confirmed the effectiveness of the coagulation-flocculation process in removing microplastics from the water. In Figure 7(h) PC2 distinguished MP-PE from MP-PP and MP-PS in the PCA score plots. The loading plot of PC2 for MP after the coagulation-flocculation process revealed that MP-PE exhibited the most significant differences from MP-PP and MP-PS at 711.68 cm^{-1} (CH rocking alkane), 2837.08 cm^{-1} (CH_3 stretching alkane), and 680.82 cm^{-1}. These positions are

critical as they correlate to the Al-O bond and further confirm the removal of microplastics through coagulation-flocculation. Additional minor differences were observed at 2950.88 cm^{-1} (CH_3 stretching), 2864.08 cm^{-1} (CH_2 stretching alkane), 1504.37 cm^{-1} (CH_2 bending alkane), 1481.22 cm^{-1} (C=C stretching), 1375.15 cm^{-1} (CH_3 stretching alkane), 1166.85 cm^{-1} and 1039.556 cm^{-1} (C-H wagging alkane), 997.13 cm^{-1} (CH_3 rocking alkane), 972.05 cm^{-1} (C–C stretching), and 730.97 cm^{-1} (C-H rocking alkane).

CONCLUSIONS

This study demonstrated the effective removal of MP-PS, MP-PE, and MP-PP—the dominant microplastics in surface waters—using coagulation–flocculation with PAC and PAM. MP-PS exhibited the highest removal efficiency, followed by MP-PE and MP-PP, with efficiency increasing alongside particle size (250–2.000 μm) and supported by near-zero zeta potential values after coagulation, confirming effective charge neutralization. Optimal conditions were achieved at pH 9, PAC = 100 mg/L, and PAM = 12–14 mg/L, while morphological, FTIR, and chemometric analyses further highlighted removal differences among MP types. These findings provide practical guidance for optimizing treatment processes and advancing sustainable water management. Nevertheless, all experiments were conducted in synthetic water, which lacks suspended solids, natural organic matter, and diverse ionic compositions typically present in surface waters—factors that can influence MP aggregation and removal, sometimes enhancing flocculation through bridging or adsorption. Moreover, only spherical MPs were tested, even though shape (fibers, fragments, spheres) strongly affects surface area, density, and hydrodynamic behavior. Future research should therefore employ realistic water matrices and diverse MP shapes to better reflect environmental conditions and improve applicability to field-scale water treatment.

Acknowledgments

We would like to express our sincere gratitude to Suranaree University of Technology for supporting this research. Special thanks are also due to KITTISIT ENTERPRISE for their support in the particle size and shape analysis conducted using the RODOS instrument.

REFERENCES

1. Adib, D., Mafifholami, R., Tabeshkia, H., Walker, T. (2022). Optimization of polypropylene microplastics removal using conventional coagulants in drinking water treatment plants via response surface methodology. *Journal of Environmental Health Science and Engineering, 20*, 565–577. https://doi.org/10.1007/s40201-022-00803-4
2. Arvaniti, O. S., Antonopoulou, G., Tsagkogianni, D., Stasinakis, A. S. (2021). Screening on the sorption of emerging contaminants to polystyrene and polyethylene and use of coagulation–flocculation process for microplastics removal. *Global NEST Journal*, 23, 303–308. https://doi.org/10.30955/gnj.003854
3. Amelia, D., Karamah, E. F., Mahardika, M., Syafri, E., Rangappa, S. M., Siengchin, S., Asrofi, M. (2022). Effect of advanced oxidation process for chemical structure changes of polyethylene microplastics. *Materials Today: Proceedings, 52*, 250–2504. https://doi.org/10.1016/j.matpr.2021.10.438
4. Chae, Y., An, Y. J. (2017). Effects of micro-and nanoplastics on aquatic ecosystems: Current research trends and perspectives. *Marine pollution bulletin*, *124*(2), 624–632. https://doi.org/10.1016/j.marpolbul.2017.01.070
5. Chavalparit, O., Ongwandee, M. (2009). Optimizing electrocoagulation process for the treatment of biodiesel wastewater using response surface methodology. *Journal of Environmental Sciences*, *21*, 1491– 1496. https://doi.org/10.1016/S1001-0742(08)62445-6.
6. Collard, F., Gasperi, J., Gabrielsen, G.W,, Tassin, B. (2019). Plastic particle ingestion by wild freshwater fish: a critical review. *Environmental Science and Technology*, *53*, 12974–12988. https://doi.org/10.1021/acs.est.9b03083
7. Colombi, C., Liebal, K., Tomasello, M., Young, G., Warneken, F., Rogers, S. (2009). Examining correlates of cooperation in autism: Imitation, joint attention, and understanding intentions. *national autistic society*, *13*(2). https://doi.org/10.1177/136236130809851
8. Duan, Y., Zhao, J., Qiu, X., Deng, X., Ren, X., Ge, W., Yuan, H. (2022). Coagulation performance and floc properties for synchronous removal of reactive dye and polyethylene terephthalate microplastics. *Process Safety and Environmental Protection*, *165*, 66–76. https://doi.org/10.1016/j.psep.2022.07.010
9. Eerkes-Medrano, D., Thompson, R.C., Aldridge, D.C. (2015). Microplastics in freshwater systems: A review of the emerging threats, identification of knowledge gaps and prioritisation of research needs. *Water Research*, *75*, 63–82. https://doi.org/10.1016/j.watres.2015.02.012
10. Egessa, R., Nankabirwa, A., Basooma, R., Nabwire, R.

(2020). Occurrence, distribution and size relationships of plastic debris along shores and sediment of northern Lake Victoria. *Environmental Pollution*, *257*, 113442. https://doi.org/10.1016/j.envpol.2019.113442

11. Fang, J., Xuan, Y., Li, Q. (2010). Preparation of polystyrene spheres in different particle sizes and assembly of the PS colloidal crystals. *Science China*, *53*(11), 3088–3093. https://doi.org/10.1007/s11431-010-4110-5
12. Fu, D., Chen, C.M., Qi, H., Fan, Z., Wang, Z., Peng, L. (2020). Occurrences and distribution of microplastic pollution and the control measures in China. *Marine pollution bulletin*, *153*, 110963. https://doi.org/10.1016/j.marpolbul.2020.110963
13. Gandurina, L.V. Gervite, É.I. (1987). Treatment of oil-containing wastewater using activated silicic acid as a flocculant. *Chemistry and Technology of Fuels and Oils*, *23*, 449–450. https://doi.org/10.1007/BF00725114
14. Gulmine, J.V., Janissek, P.R., Heise, H.M., Akcelrud, L. (2002). Polyethylene characterization by FTIR. *Polymer Testing*, *21*, 557–563. https://doi.org/10.1016/S0142-9418(01)00124-6
15. Hassan, M., Nour, M., Abdelmonem, Y., Makhlouf, G., Abdelkhalik, A. (2016). Synergistic effect of chitosan-based flame retardant and modified clay on the flammability properties of LLDPE. *Polymer Degradation and Stability*, *133*, 8–15. https://doi.org/10.1016/j.polymdegradstab.2016.07.011
16. Huang, J.S., Koongolla, B., Li, H.X., Lin, L., Pan, Y.F., Liu, S., He, W.H., Maharana, D., Xu, X.R. (2020). Microplastic accumulation in fish from Zhanjiang mangrove wetland, South China. *Science of The Total Environment*, *708*, 134839. https://doi.org/10.1016/j.scitotenv.2019.134839
17. Jiang, J.Q., Panagoulopoulos, A., Bauer, M., Pearce, P. (2006). The application of potassium ferrate for sewage treatment. *Journal of Environmental Management*, *79*, 215–220. https://doi.org/10.1016/j.jenvman.2005.06.009
18. Julian, C., Bernhard, P.K., Kiel, B.P., Eberhard, J., Schmidt, S., Kaltschmidt, C., Kaltschmidt, B., Hutten, A., Anselmetti, D. (2023). Aging of industrial polypropylene surfaces in detergent solution and its consequences for biofilm formation. *Polymers, 15*(5), 1247. https://doi.org/10.3390/polym15051247
19. Kabsch-Korbutowicz M. (2005). Effect of Al coagulant type on natural organic matter removal efficiency in coagulation/ultrafiltration process. *Desalination*, 185, 327–333. https://doi.org/10.1016/j.desal.2005.02.083
20. Lei, L., Wu, S., Lu, S., Liu, M., Song, Y., Fu, Z., Shi, H., Raley-Susman, K.M., He, D. (2018). Microplastic particles cause intestinal damage and other adverse effects in zebrafish Danio rerio and nematode Caenorhabditis elegans. *Science of The Total Environment*, 619–620, 1–8. https://doi.org/10.1016/j.scitotenv.2017.11.103
21. Lin, J.H., Pan, Y.J., Liu, C.F., Huang, C.L., Hsieh, C.T., Chen, C.K., Lin, Z.L., Lou, C.W. (2015). Preparation and compatibility evaluation of polypropylene/high density polyethylene polyblends. *Journal of Applied Polymer Science*, *132*(25), 42675. https://doi.org/10.3390/ma8125496
22. Luo, H., Liu, C., He, D., Sun, D., Zhang, A., Li, J., Pan, X. (2022). Interactions between polypropylene microplastics (PP-MPs) and humic acid influenced by aging of MPs. *Water research, 222*, 1189221. https://doi.org/10.1016/j.watres.2022.118921
23. Ma, B., Xue, W., Hu, C., Liu, H., Qu, J., Li, L. (2019b). Characteristics of microplastic removal via coagulation and ultrafiltration during drinking water treatment. *Chemical Engineering Journal*, *359*, 159–167. https://doi.org/10.1016/j.cej.2018.11.155
24. Mcyotto, F., Wei, Q., Macharia, D.K., Huang, M., Shen, C., Chow, C.W.K. (2021). Effect of dye structure on color removal efficiency by coagulation. *Chemical Engineering Journal*, 405, 126674. https://doi.org/10.1016/j.cej.2020.126674
25. Mikulec, V., Adamović, P., Cvetković, Ž., Ivešić, M., Kljusurić, J.G. (2023). Green techniques for detecting microplastics in marine with emphasis on FTIR and NIR spectroscopy-short review. *Processes, 11*(8), 2360. https://doi.org/10.3390/pr11082360
26. Moura, D.S., Pestana, C.J., Moffat, C.F., Hui, J., Irvine, J.T.S., Lawton, L.A. (2023). Characterisation of microplastics is key for reliable data interpretation. *Chemosphere*, *331*(2023), 138691. https://doi.org/10.1016/j.chemosphere.2023.138691
27. Pedro, C., Fionn, M. (2015). Hierarchical Clustering. *1st Edition*. Chapman and Hall/CRC, New York.
28. Peller, J.R., Mezyk, S.P., Shidler, S., Castleman, J., Kaiser, S., Faulkner, R.F., Pilgrim, C.D., Wilson, A., Martens, S., Horne, G.P. (2022). Facile nanoplastics formation from macro and microplastics in aqueous media. *Environmental Pollution*, *313*, 120171. https://doi.org/10.1016/j.envpol.2022.120171
29. Pivokonsky, M., Cermakova, L., Novotna, K., Peer, P., Cajthaml, T., Janda, V. (2018). Cajthaml, T., Janda, V., Occurrence of microplastics in raw and treated drinking water. *Environmental Science and Technology, 643*, 10188–10196. https://doi.org/10.1016/j.scitotenv.2018.08.102
30. Shahi, N.K., Maeng, M., Kim, D., Dockko, S. (2020). Removal behavior of microplastics using alum coagulant and its enhancement using polyamine-coated sand. *Process Safety and Environmental Protection. 141*, 9–17.
31. Silverstein, M.S,, Shach-caplan, M., Bauer, B.J., Hedden, R.C., Lee, H.J., Landes, B.G. (2005). Nanopore Formation in a Polyphenylene Low-k

Dielectric. *Macromolecules*, *38*(10), 4301–4310. https://doi.org/10.1021/ma047353

32. Skaf, D.W., Punzi, V.L., Rolle, J.T., Kleinberg, K.A. (2020). Removal of micron-sized microplastic particles from simulated drinking water via alum coagulation. *Chemical Engineering Journal*, *386*, 123807. https://doi.org/10.1016/j.cej.2019.123807
33. Stanton, T., Johnson, M., Nathanail, P., MacNaughtan, W., Gomes, R. L. (2020). Freshwater microplastic concentrations vary through both space and time. *Environmental Pollution*, *263*, 114481. https://doi.org/10.1016/j.envpol.2020.114481
34. Summers, S., Henry, T., Gutierrez, T. (2018). Agglomeration of nano- and microplastic particles in seawater by autochthonous and de novo-produced sources of exopolymeric substances. *Marine pollution bulletin*, 130, 258–267. https://doi.org/10.1016/j.marpolbul.2018.03.039
35. Tabatabaei, F., Mafigholami, R., Moghimi, H., Khoramipoor, S. (2023). Effect of Fe and Al based coagulants and disinfectants on polyethylene microplastics removal in coagulation process through response surface methodology. *Water Science Technology*, *87*(1), 99. https://doi.org/10.2166/wst.2022.393
36. Tong, H., Jiang, Q., Hu, X., Zhong, X. (2020). Occurrence and identification of microplastics in tap water from China. *Chemosphere, 252*, 126493. https://doi.org/10.1016/j.chemosphere.2020.126493
37. Wagner, H., Finkenzeller, T., Würth, S., Duvillard, S.P.V. (2014). Individual and team performance in team-handball: A review. *Journal of Sports Science and Medicine*, *13*(4), 808–816.
38. Wang, S., Li, E., Li, J., Du, Z., Cheng, F. (2020). Preparation and coagulation-flocculation performance of covalently bound organic hybrid coagulant with excellent stability. *Colloids and Surfaces A: Physicochemical and Engineering Aspects*, *600*, 124966. https://doi.org/10.1016/j.colsurfa.2020. 124966
39. Wei, N., Zhang, Z., Liu, D., Wu, Y., Wang, J., Wang, Q. (2015). Coagulation behavior of polyaluminum chloride: Effects of pH and coagulant dosage. *Chinese Journal of Chemical Engineering, 23*(6), 1041–1046. https://doi.org/10.1016/j.cjche.2015.02.003
40. Weinstein, J.E., Crocker, B.K., Gray A.D. (2016). From macroplastic to microplastic: Degradation of high-density polyethylene, polypropylene, and polystyrene in a salt marsh habitat. *Environmental Toxicology and Chemistry.* https://doi.org/10.1002/etc.3422
41. Wiśniewska, M., Chibowski, S., Urban, T. (2015). Impact of anionic and cationic polyacrylamide on the stability of aqueous alumina suspension—comparison of adsorption mechanism. *Colloid and Polymer Science*, *293*, 405–411. https://doi.org/10.1007/s00396-015-3509-8
42. Xu, P., Peng, G., Su, L., Gao, Y., Gao, L., Li, D. (2018b). Microplastic risk assessment in surface waters: a case study in the Changjiang Estuary, China. *Marine pollution bulletin, 133*, 647–654. https://doi.org/10.1016/j.marpolbul.2018.06.020
43. Yang, Z., Gao, B., Cao, B., Xu, W., Yue, Q. (2011). Effect of OH^-/Al^{3+} ratio on the coagulation behavior and residual aluminum speciation of polyaluminum chloride (PAC) in surface water treatment. *Separation and Purification Technology*, *80*(1), 59–66. https://doi.org/10.1016/j.seppur.2011.04.007
44. Yin, L., Wen, X., Huang, D., Zeng, G., Deng, R., Liu, R., Zhou, Z., Tao, J., Xiao, R., Pan, H. (2021). Microplastics retention by reeds in freshwater environment. *Science of The Total Environment*, *790*, 148200. https://doi.org/10.1016/j.scitotenv.2021.148200
45. Zhang, Y., Zhou, G., Yue, J., Xing, X., Yang, Z., Wang, X., Wang, Q., Zhang, J. (2021). Enhanced removal of polyethylene terephthalate microplastics through polyaluminum chloride coagulation with three typical coagulant aids. *Science of The Total Environment, 800*, 149589. https://doi.org/10.1016/j.scitotenv.2021.149589
46. Zhao, Y., Yuan, H., He, Y., Cheng, C. (2022). Effect of Hydroxyl Aluminum Ratio on Preparation of PAC from Aluminum Ash. *In Proceedings of the 3rd International Symposium on Water, Ecology and Environment*. 106–110.
47. Zhao, Z., Pan, S., Ye, Y., Zhang, X., Pan, B. (2020). FeS_2/H_2O_2 mediated water decontamination from p-arsanilic acid via coupling oxidation, adsorption and coagulation: Performance and mechanism. *Chemical Engineering Journal*, *381*, 122667. https://doi.org/10.1016/j.cej.2019.122667
48. Zhou, G., Wang, Q., Li, J., Li, Q., Xu, H., Ye, Q., Wang, Y., Shu, S., Zhang, J. (2021). Removal of polystyrene and polyethylene microplastics using PAC and $FeCl_3$ coagulation: performance and mechanism. *Science of The Total Environment, 752*, 141837. https://doi.org/10.1016/j.scitotenv.2020.141837
49. Zocchi, M., Sommaruga, R. (2019). Microplastics modify the toxicity of glyphosate on Daphnia magna. *Science of the Total Environment, 697*, 134194. https://doi.org/10.1016/j.scitotenv.2019.134194